Est. 1984

ORIENTAL JOURNAL OF CHEMISTRY
An International Open Access, Peer Reviewed Research Journal

www.orientjchem.org

ISSN: 0970-020 X
CODEN: OJCHEG
2022, Vol. 38, No.(2):
Pg. 312-317

Hydrothermal Synthesis and Characterization of Yttrium oxide nanoparticles: Bioavailability and Targeting of Breast Tumors

G. MYVIZHI[1] and S. K. KRISHNA[2]*

Department of Chemistry, Chickkaiah Naicker College, Erode-638 004,Tamilnadu, India.
*Corresponding author E-mail: raghul2022@gmail.com

http://dx.doi.org/10.13005/ojc/380211

(Received: December 08, 2021; Accepted: March 13, 2022)

ABSTRACT

Herein, we describe synthesis of Yttrium Oxide (yttria) nanoparticles of 0.1, 0.2, 0.3 and 0.4 M concentrations by hydrothermal method and characterized using various techniques. Powder XRD analysis showed that the as-prepared nanoparticles have cubic Y_2O_3 structure with an average crystallite diameter of 34-58 nm. SEM micrographs depicted that agglomerated yttria nanoparticles of different morphological properties and particles in size. The occurrence of metal oxide is affirmed using FTIR and EDX analysis. The Yttrium oxide nanoparticles showed better antimicrobial activity against ADCP declared harmful bacteria pathogens such as *E. coli, S. paratyphi, S. aureus*, and *S. pyogenes*. Further, the yttrium oxide nanoparticles revealed better anticarcinogenic activity against MCF-7 cell line with IC_{50} value 47.07 µg/mL. From these findings, the nanoparticles of Y_2O_3 are candidates to be used as potential alternatives in antitumor therapy.

Keywords: Nanostructures, Oxides, Hydrothermal synthesis, X-ray diffraction, Biological applications.

INTRODUCTION

The serendipity discovery of nano size rare earth metal oxide particles are concerned because of their notable developments and its idiosyncratic nature. Synthesis of nanoparticles is becoming a new challenge in the improvement of advanced functional materials for the reason that they exhibit unique properties deliberate by particles of very small dimension in contrast to the related bulk material[1-5]. Rare earth nanomaterials, in different structures such as nanoparticles, wires, flowers, tubes, needles and nanocrystals have fascinating physicochemical characteristics which be different from their micro counterparts and that draw a great deal of attention. These materials are widely used in diverse fields. In earlier reports, rare earth nanomaterials have attractive physico-chemical applications. These rare earth oxide nano materials have been used various fields for prosper new devices[6,7]. Yttrium oxide (yttria) have been widely used rare earth among rare earth Oxides which actively studied in the recent years and it exists in three crystallite phases including cubic, hexagonal and monoclinic. Major properties of yttria and yttria based material rely upon the crystalline form of the material and the imperfections existing inside the material[8]. Because of its excellent properties like high refractory accomplishment, thermal conductivity, superior chemical stability many researchers have tried to synthesise yttrium

based nanomaterials in recent years. Yttria has an extensive transparency altering from violet to infrared range. Yttrium oxide improved strength and toughness of the ceramic materials. It is also used as alternative for SiO_2 because of its dielectric characteristic[9-11]. Yttria nanoparticles have been readily synthesised by variety of methods such as microemulsion, pyrolysis, evaporation-condensation and ultrasonic irradiation synthesis[12-13]. Hence, in this study we have explored low cost hydrothermal preparation of yttrium oxide nanoparticles of different morphologies using various precursor concentrations and then uses these nanoparticles to evaluate *in vitro* cytotoxicity on MCF-7 breast cancer cell line by MTT assay method and their bioavailability.

MATERIALS AND METHODS

In this study, the precursor material used was Yttrium nitrate hexa hydrate $Y(NO_3)_3.6H_2O$ (99.8% purity) which was obtained from Merck. In the preparation of yttrium oxide nanoparticles, KOH employed as a precipitating agent which was purchased from Alfa aesar. All of the chemicals were of analytical grade and were used without further purification. The nanocrystalline yttrium oxide powders are prepared by hydrothermal method.

The yttrium oxide nanoparticles were prepared via hydrothermal process. About 10 mL of $Y(NO_3)_3.6H_2O$ (0.1 M) was taken in a 100 mL beaker. Meanwhile, 80 mL of 10% KOH was added and stirred vigorously for 1 h to make homogeneous solution. Then the homogeneous mixture was autoclaved at the temperature 180°C for 6 h with alkaline medium in 50 mL teflon lined autoclave. Then the autoclave was cooled. The final solution was centrifuged and washed several times with distilled water and ethanol and subsequently dried at 100°C for 2 h using vacuum oven. Then obtained final product was collected in a silica crucible and calcined to 500°C for 3 h in muffle furnace for preparing the yttrium oxide nanoparticles. Followed the same steps for 0.2, 0.3 and 0.4 M samples were prepared and characterized.

Characterization

The phase purity and crystallite nature of the synthesised samples were determined using powder X-ray diffraction (XRD) using Bruker AXS D8 advance X-ray diffractometer instrument. The morphological properties of the powder nanoparticles was characterized by SEM equipped with EDAX EDS detector (Leo, Germany) at an accelerating voltage of 10 kV. The UV-Vis spectra were recorded by using a Shimadzu spectrophotometer (UV-1700) to measure the band gap in the synthesised sample. The photoluminescence were examined by Cary Eclipse Spectrofluorophotometer under excitation wavelength of 280nm. The surface functional groups were determined by Perkin-Elmer Spectrophotometer in the spectral range of 4000 cm^{-1}-400 cm^{-1}.

Antimicrobial susceptibility test: Agar diffusion method

The antibacterial activity of Yttrium oxide nanoparticles was determined using agar diffusion method. Two *Gram-negative* (Salmonella paratyphi and *Escherichia coli*) and two *Gram-positive* (*Staphylococcus aureus* and *Streptococcus pyogenes*) bacterial strains were used. Briefly, about 10 μl test samples at different concentrations was used against each strain swabbed on nutrient agar plates and then incubated at 37°C for 24 hours. Chloramphenicol (10 μg) was used as standard. After the incubation period the zone of inhibition was measured against tested pathogens[14].

Anticancer Analysis: MTT ASSAY

To determine the cytotoxic effect of Yttrium nanoparticles, cell viability study was carried out with MTT reduction assay. MCF-7 cells were seeded in 96-well plate at the density $1x10^5$ cells/well. The cells were allowed to grown in 96-well plate for 24 h with 5% FBS. After that, the media was removed and replaced with a suspension of various concentrations of Yttrium nanoparticles were incubated for 48 hours. After incubation, about 15 μl of MTT (5 mg/mL) in phosphate buffered saline (PBS) was added and incubated at 37°C for 4 hours. The medium with MTT was then flicked off and the formed formazan crystals were solubilized in 100 μL of DMSO. The absorbance of the formazan product was recorded at 510nm using micro plate reader[15-16].

RESULTS AND DISCUSSION

Powder XRD analysis

The Powder XRD patterns of yttrium oxide nanoparticles synthesised using hydrothermal method are shown Fig.1. The XRD pattern for

the samples depict that the characteristic peaks are well consistent in agreement with the JCPDS card, given that further formation of Yttrium oxide nanoparticles are confirmed. Further, synthesized Yttrium oxide is cubic and good crystalline in nature. In all the samples, the most important peaks are observed to various (hkl) planes with no additional peaks and are well consistent with JCPDS: No: 41-1105[17]. Apart from that, the crystallinity for yttrium oxide is improved when the molar concentration increases. The crystallite size 'D' of the samples are evaluated using Scherrer's formula from the XRD line broadening measurement

$$D = K\lambda/(\beta Cos\theta)$$

The average crystallite size is found to be in the range 34, 38, 52 and 58 nm for 0.1, 0.2, 0.3 and 0.4 M samples. The crystallite size increases with sample concentration.

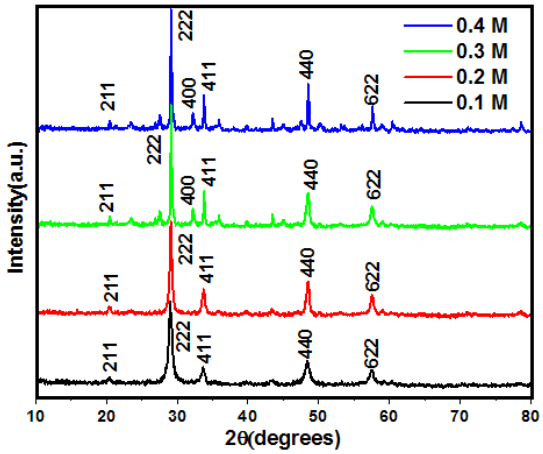

Fig. 1. PXRD pattern of Yttrium Oxide nanoparticles

The characteristic Bragg diffractions at 2θ values approximately 20.42°, 29.10°, 33.77°, 48.50° and 57.45° are indexed to the (211), (222), (400), (440) and (622) planes, respectively by comparison with JCPDS card No. 41-1105[18]. The distinct and sharp reflection peaks signify that the synthesised yttrium oxide nanoparticles posses high crystallinity and purity.

FTIR analysis

Figure 2 depicts the FTIR spectra of yttrium oxide nanoparticles for diverse precursor concentration. The FTIR spectra for all the samples, the strong band at 3496, 3498, 3500 and 3538 cm^{-1} are associated with –OH stretching vibration mode. Subsequently, the weak band at 1712, 1770, 1778 and 1804 cm^{-1} is assigned to the deformation mode of –OH group. The peaks observed at 1550, 1552, 1577 and 1579 cm^{-1} are owing to the different vibration of carboxylate group which may due to the absorption of CO_2 when exposed to air. Conversely all the other characteristic peaks for yttrium oxide is found in this spectrum. The peaks at 902, 867, 865 and 864 cm^{-1} associated with Y-OH stretching vibration of Yttrium hydroxide. The spectrum of yttrium oxide confirms that the intensity of OH and CO_3^{2-} groups reduce remarkably. Besides, a new absorption peaks at 602, 584, 578 and 574 cm^{-1} are found which is assigned to Y-O stretching mode signifying the formation of yttrium oxide nanoparticles from Yttrium hydroxide[17-19].

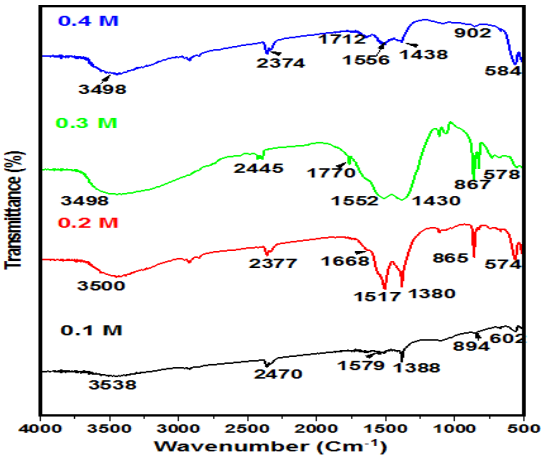

Fig. 2. FTIR spectra of Yttrium Oxide nanoparticles

Electron microscopy with EDAX analysis

Figure 3 shows the morphological images of the as-synthesised yttrium oxide nanoparticles obtained using various precursor concentration. The micrograph obtained for low precursor concentration resembles that they are in nanoscale and needle like structure homogeneously with discrete in nature (Fig. 3a & 3b). Whereas, the morphology of yttrium oxide nanoparticles prepared from high molar concentration shows varied size and shape with void and more agglomeration shown in Fig. 3c & 3d. Obviously the size of the nanoparticles increased owing to increase in precursor concentration which was also affirmed by Scherrer's equation. Further, EDX analysis revealed that occurrence of the characteristic and distinct line of Yttrium (Y) and oxygen (O) signal of the yttrium oxide nanoparticles and there is no impurities were occurrence in the synthesized materials. Hence the morphological

results portray clearly that the nanoparticles obtained from low precursor concentrations having well defined morphological properties with uniform shape and less agglomeration[20].

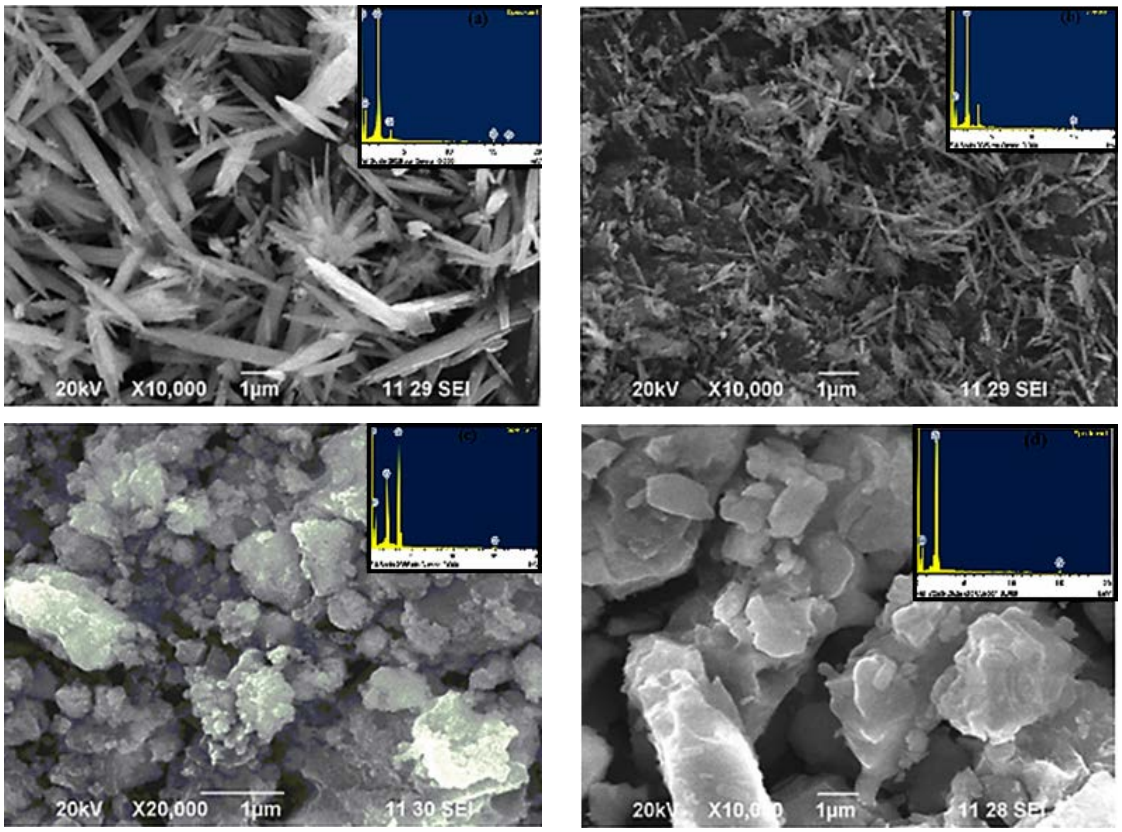

Fig. 3 (a-d). SEM with EDX images of Yttrium Oxide nanoparticles

Table 1: Zone of Inhibhition of Yttrium Oxide nanoparticles against test organism

S.No	Pathogenic bacteria	Zone of inhibition (mm)*			Standard (Chloramphenicol)
		10 μg	20 μg	30 μg	
1	*Staphylococcus aureus*	N	03	06	12
2	*Streptococcus pyogenes*	N	03	05	10
3	*Escherichia coli*	N	05	06	10
4	*Salmonella paratyphi*	N	04	06	12

*Values are means of triplicates (n=3), N- no zone of inhibition was found

Antibacterial activity

The antibacterial activity of as-synthesised 0.1 M yttrium oxide nanoparticles were assessed adjacent to *Staphylococcus aureus, Streptococcus pyogenes, Escherichia coli* and *Salmonella paratyphi* at a concentration 10 μg, 20 μg, 30 μg and chloramphenicol as control.

As stated in Table 1 and Fig. 4 the zone of inhibition of pathogenic microorganisms increases when the concentration of Yttrium oxide increases which lends to previous reports in the literature that the activity was directly proportional to the concentration of nanoparticles. The positive control Chloramphenicol (10 μg $disc^{-1}$) used in this study exhibited a zone of inhibition in the range of 10 mm to 12 mm against test pathogens. Moreover, the results clearly demonstrate that *E. coli* and *S. paratyphi* strains were more susceptible to the studied compounds than *Staphylococcus aureus* and *Streptococcus pyogenes*. Further, *Gram-negative* microbial strains offered a zone of inhibition from 4 mm to 6 mm owing to having difference in cell wall membranes and peptidogly can between outer

and inner membrane, and easily these substances enhance the penetration of the nanocomposite material into the cells. Possible mechanism for the antibacterial activity of yttrium oxide nanoparticles are based on the metal ion enter through the cell membrane causing massive leakage of intracellular substances and eventually causing cell death of the pathogens[21]. Hence the results indicate that as-prepared Yttrium oxide nanoparticles could be used to control the pathogenic microorganisms.

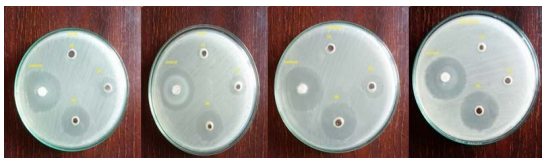

Fig. 4. Images of Yttrium Oxide Nanoparticles adjacent to *Staphylococcus aureus, Streptococcus pyogenes, E. coli* and *Salmonella paratyphi*

Anticancer analysis

The *in vitro* anticancer activity of 0.1 M Yttrium oxide nanoparticles were analysed with the human breast cancer cell line MCF-7 were examined at diverse concentrations (6.5, 12.5, 25, 50 and 100 µg mL^{-1}). The percentage of cell inhibition for yttrium oxide is given in Fig. 5 and Fig. 6 depicts the microscopic images of 0.1 M yttrium oxide nanoparitcles.

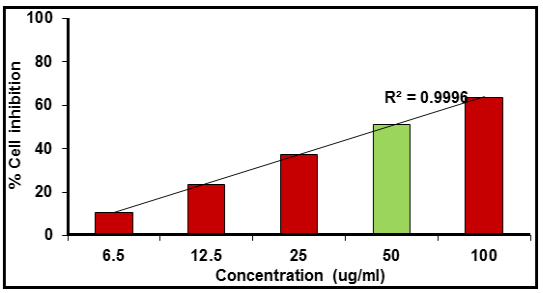

Fig. 5. Percentage of cancer cell inhibition for Yttrium Oxide nanoparticles

IC_{50} values calculated from nonlinear decay Fig. 5 were plot between the % of Cell inhibition and log concentration and IC_{50} was evaluated using Graph Pad Prism software. From this analysis, it is confirmed that even a higher concentration of the sample (100 µg/mL) inhibit growth of more cancerous cells. It is significant that prepared samples exhibited much higher cytotoxic effect against breastic cancer (MCF) cell line (Inhibition ratio more than 63.63%) with the determined IC_{50} values 47.07 µg/mL. In fact, Yttrium nanoparticles may stimulate reactive oxygen species and significantly inhibiting the growth of cellular compounds which lead to cell death[22]. The finding results thus indicated that the prepared yttrium oxide nanoparticles has antitumor activity might be a potential alternative agent for human breast cancer therapy.

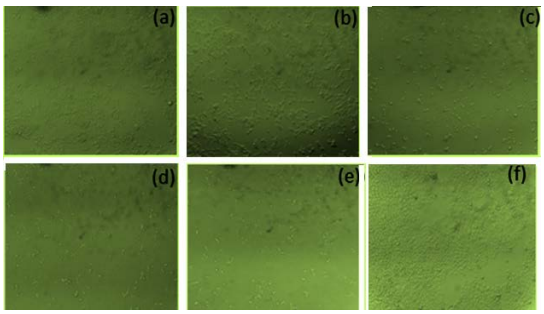

Fig. 6. Micrographic images of Cell viability in human breast (MCF-7) cells determined by MTT assay with diverse concentrations(a-e), Control(f)

CONCLUSION

In Summary, Nanocrystalline yttria has been effectively prepared by low cost hydrothermal technique. The XRD results confirmed that yttria nanoparticles were cubic phase and crystallite size varies from 34–58 nm. The FTIR results confirmed that the formation of yttrium oxide nanoparticles and were found to be pure. The SEM images demonstrated that the precursor concentration of yttria plays a major role in controlling the morphology and size of the nanoparticle and hence the optimum concentration was found to be 0.1 M. Further, the as-prepared yttrium oxide nanoparticles showed improved antimicrobial activity against pathogenic microorganisms. The prepared Yttrium Oxide nanoparticles were assayed for their anticancer activity and the obtained results proved their anticancer behaviour. Hence, cytotoxic effect of this study suggests the possibility of trying the use of prepared Yttrium Oxide nanoparticles as anticancer drugs.

ACKNOWLEDGMENT

This research did not receive any specific grant from funding agencies in the public, commercial, or not-for-profit sectors.

Conflict of Interest

The authors declare that there is no conflict of interests regarding the publication of this article.

REFERENCES

1. Ariga, K.; Hill, J. P.; Lee, M. V.; Vinu, A.; Charvet, R.; Acharya, S. *Sci. Technol. Adv. Mater.*, **2008**, *9*(1).
2. Yi, G. S.; Chow, G. M. Colloidal LaF3:Yb,Er, LaF3:Yb,Ho and LaF 3:Yb, Tm *J. Mater. Chem.*, **2005**, *15*(41), 4460–4464.
3. Stouwdam, J. W.; Van Veggel, F. C. *J. M. Nano Lett.*, **2002**, *2*(7), 733–737.
4. Gao, X.; Cui, Y.; Levenson, R. M.; Chung, L. W. K.; Nie, S. *Nat. Biotechnol.*, **2004**, *22*(8), 969–976.
5. Åkerman, M. E.; Chan, W. C. W.; Laakkonen, P.; Bhatia, S. N.; Ruoslahti, E. *Proc. Natl. Acad. Sci. U. S. A.*, **2002**, *99*(20), 12617–12621.
6. Gao, X.; Yang, L.; Petros, J. A.; Marshall, F. F.; Simons, J. W.; Nie, S. *Curr. Opin. Biotechnol.,* **2005**, *16*(1 SPEC. ISS.), 63–72.
7. Jamalaiah, B. C.; Kumar, J. S.; Babu, A. M.; Moorthy, L. R. *J. Alloys Compd.*, **2009**, *478* (1–2), 63–67.
8. Cao, Y. C. 1046. *J. Am. Chem. Soc.*, **2004**, *126*, 7456. Pdf. 2004, No. Fig. 2, 7456–7457.
9. Graeve, O. A.; Varma, S.; Rojas-George, G.; Brown, D. R.; Lopez, E. A. *J. Am. Ceram. Soc.,* **2006**, *89*(3), 926–931.
10. Towata, A.; Sivakumar, M.; Yasui, K.; Tuziuti, T.; Kozuka, T.; Iida, Y. *J. Mater. Sci.*, **2008**, *43* (4), 1214–1219.
11. Mokkelbost, T.; Kaus, I.; Grande, T.; Einarsrud, M. A. *Chem. Mater.*, **2004**, *16*(25), 5489–5494.
12. Srinivasan, R.; Yogamalar, N. R.; Elanchezhiyan, J.; Joseyphus, R. J.; Bose, A. C. *J. Alloys Compd.*, **2010**, *496*(1–2), 472–477.
13. da Silva, C. A.; Ribeiro, N. F. P.; Souza, M. M. V. M. *Ceram. Int.*, **2009**, *35*(8), 3441–3446.
14. K. Shimada, K. Fujikawa, K. Yahara, and T. Nakamura, *J. Agric. Food Chem.*, 1992, *40*(6), 945–948.
15. Mosmann, T, *Journal of Immunological Methods.*, **1983**, *65*, 55-63.
16. Monks, A.; Scudiero, D.; Skehan, P.; Shoemaker, R.; Paull, K.; Vistica, D.; Hose, C.; Langley, J.; Cronise, P.; Vaigro-Wolff, A.; Gray-Goodrich, M.; Campbell, H.; Mayo, J.; Boyd., **1991**.
17. Srinivasan, R.; Yogamalar, R.; Bose, A. C. *Mater. Res. Bull.*, **2010**, *45*(9), 1165–1170.
18. Liu, X.; Zhou, F.; Gu, M.; Huang, S.; Liu, B.; Ni, C. *Opt. Mater. (Amst).,* **2008**, *31*(2), 126–130.
19. Konrad, A.; Herr, U.; Tidecks, R.; Kummer, F.; Samwer, K. *J. Appl. Phys.*, **2001**, *90*(7), 3516–3523.
20. Blaskovich, M. A. T.; Kavanagh, A. M.; Elliott, A. G.; Zhang, B.; Ramu, S.; Amado, M.; Lowe, G. J.; Hinton, A. O.; Pham, D. M. T.; Zuegg, J.; Beare, N.; Quach, D.; Sharp, M. D.; Pogliano, J.; Rogers, A. P.; Lyras, D.; Tan, L.; West, N. P.; Crawford, D. W.; Peterson, M. L.; Callahan, M.; Thurn, M. *Commun. Biol.*, **2021**, *4*(1).
21. Jeevanandam, J.; Barhoum, A.; Chan, Y. S.; Dufresne, A.; Danquah, M. K. Beilstein *Journal of Nanotechnology. Beilstein-Institut Zur Forderung der Chemischen Wissenschaften.*, **2018**, 1050–1074.
22. Wang, L.; Hu, C.; Shao, L. *Int. J. Nanomedicine.,* **2017**, *12*, 1227–1249.